Late-life restoration of mitochondrial function reverses cardiac dysfunction in old mice

[1,2]Ying Ann Chiao, [1]Huiliang Zhang, [1]Mariya Sweetwyne, [1]Jeremy Whitson, †[3]Ying Sonia Ting, [4]Natan Basisty, [3]Lindsay Pino, [1]Ellen Quarles, [1]Ngoc-Han Thi Nguyen, [5]Matthew D. Campbell, [6]Tong Zhang, [6]Matthew J. Gaffrey, [3]Gennifer Merrihew, [7]Lu Wang, [8]Yongping Yue, [8]Dongsheng Duan, [9]Henk Granzier, [10]Hazel H. Szeto, [6]Wei-Jun Qian, [5]David Marcinek, [3]Michael J. MacCoss and [1]Peter S. Rabinovitch.

[1]Department of Pathology, University of Washington, Seattle, WA, USA
[2]Aging and Metabolism Program, Oklahoma Medical Research Foundation
[3]Department of Genome Science, University of Washington, Seattle, WA, USA
[4]Buck Institute of Aging Research
[5]Department of Radiology, University of Washington, Seattle, WA, USA
[6]Biological Sciences Division, Pacific Northwest National Laboratory
[7]Department of Environmental and Occupational Health Sciences, University of Washington, Seattle, WA, USA
[8]Department of Molecular Microbiology and Immunology, School of Medicine, University of Missouri
[9]Department of Cellular and Molecular Medicine, University of Arizona
[10]Social Profit Network, Menlo Park
†Deceased May 23, 2019, with the article dedicated to her memory

Correspondence:
Peter S. Rabinovitch, MD, PhD
Department of Pathology, University of Washington
1959 NE Pacific St., HSB-K081, Seattle, WA 98195
Phone: 206-685-3761; Fax: 206-616-8271
Email: petersr@u.washington.edu

Abstract

Mitochondrial dysfunction is a hallmark of aging but whether restoration of mitochondrial function can reverse pre-existing age-related diseases is not well-established. Diastolic dysfunction is a prominent feature of cardiac aging in both mice and humans, and we show here that 8-week treatment with the mitochondrial targeted peptide SS-31 (elamipretide) can substantially reverse this deficit in old mice. Mechanistically, SS-31 treatment normalized the increase in proton leak and reduced mitochondrial ROS in cardiomyocytes from old mice; these cellular changes were accompanied by reduced protein oxidation and a shift towards a more reduced protein thiol redox state in old hearts. The improvement in diastolic function was associated with increased phosphorylation at Ser282 of cMyBP-C but was independent of titin isoform shift. SS-31 treatment cannot further improve cardiac function of old mice that express mitochondrial-targeted catalase (mCAT), implicating normalizing mitochondrial oxidative stress as an overlapping mechanism. Late-life viral expression of mCAT produced similar functional benefits in old mice, further indicating that reduction of mitochondrial ROS as a critical mechanism. Despite their similar functional benefits, SS-31 and mCAT differentially regulated cMyBP-C and cTnI phosphorylation, suggesting divergence of mechanisms downstream of mitochondrial ROS reduction. Overall, these results demonstrate that pre-existing cardiac aging phenotypes can be reversed by targeting mitochondrial dysfunction and implicate mitochondrial energetics and redox signaling as therapeutic targets of cardiac aging.

Introduction

Mitochondrial dysfunction is one of the hallmarks of aging [1]. While mitochondria generate the bulk of cellular ATP, they are also the major source of reactive oxygen species (ROS) in most cells. The mitochondrial free radical theory of aging proposes that excessive mitochondrial ROS damages mitochondrial DNA and proteins, and this leads to further mitochondrial dysfunction, with subsequent cellular and organ functional declines and limits on lifespan and healthspan [2].

Aging is the strongest risk factor for cardiovascular diseases [3]. It is also accompanied by a decline in cardiac function, especially diastolic dysfunction and hypertrophy of the left ventricle and left atrium [4]. The heart is rich in mitochondria and has a high metabolic demand; therefore, it is highly susceptible to oxidative damage and the effects of mitochondrial dysfunction. Increasing evidence suggests that mitochondrial oxidative stress and mitochondrial dysfunction play critical roles in cardiovascular diseases and cardiac aging [5].

The therapeutic potential of reducing mitochondrial oxidative stress is supported by mice expressing mitochondrial-targeted catalase (mCAT) [6]. In these mice, catalase removes hydrogen peroxide in mitochondria and significantly reduces mitochondrial protein oxidative damage and mitochondrial DNA mutation and deletion frequencies in mCAT mice. In addition to an extension of median and maximum lifespan, mCAT mice displayed greatly attenuated cardiac aging phenotypes, including reduced cardiac hypertrophy and improved diastolic function and myocardial performance [7]. Expression of mCAT is also protective in models of cardiac hypertrophy and failure [8]. These cardiac benefits suggest that pharmacologic interventions combating mitochondrial ROS and improving mitochondrial function are attractive targets for treatment of cardiovascular disease and cardiac aging. We focused on the mitochondrial-targeted tetrapeptide SS-31 (elamipretide), as it was previously shown to prevent pressure overload-induced cardiac hypertrophy and failure in a manner that was highly similar to mCAT [9-11]. While these and other studies have shown that combating mitochondrial ROS during the course of a lifetime or during work and pressure overload stress can prevent mitochondrial dysfunction and attenuate cardiac functional decline [12, 13], it has not been established whether delivering such interventions in later life can rescue pre-existing mitochondrial and cardiac dysfunction. In this study, we demonstrate that mitochondrial targeted interventions can improve mitochondrial function and reverse pre-existing cardiac dysfunction in old mice.

Results

8-weeks SS-31 treatment rescues cardiac dysfunction and hypertrophy in old mice

Diastolic function and myocardial performance decline significantly with age [7, 14, 15]. Compared to young mice, old mice exhibit a reduced ratio of early to late diastolic mitral annulus velocities (Ea/Aa), indicating a decline in diastolic function, and they have an increased (poorer) myocardial performance index (MPI), indicating an increased fraction of the cardiac cycle that is not accompanied by a change in volume [7, 14, 15]. To determine the effects of SS-31 treatment on cardiac function in old mice, we treated 24-month-old mice with the SS-31 peptide or saline control and examined cardiac function by echocardiography after 4 and 8 weeks of treatment. We found that Ea/Aa increased and MPI decreased in old mice treated with SS-31 for 4 or 8 weeks, reversing the age-related changes, and both parameters were significantly different compared to saline controls at 8 weeks of treatment (Fig. 1a, b). Systolic function, measured as fractional shortening, was similar between old control and old SS-31 treated mice (Fig. 1c). At the 8-week necropsy, we observed a higher heart weight normalized to tibia length (HW/TL) in old control mice, but not in old SS-31 treated mice, compared to young control mice (Fig. 1d), suggesting a regression of age-related cardiac hypertrophy after SS-31 treatment. As in male

mice, we observed a similar improvement in Ea/Aa in 24-month old female mice treated with SS-31 for 8 weeks (Fig. 1e), suggesting that the treatment is effective in both sexes. To evaluate the persistence of the SS-31 induced cardiac benefit, we continued to monitor cardiac function in these mice after cessation of treatment. We found that the improved Ea/Aa in SS-31 treated mice was maintained at 2 weeks, but dropped by approximately half at 4 weeks after treatment ceased (Fig. 1e). A decline in diastolic cardiac function in the elderly is associated with exercise intolerance, so we studied whether exercise performance was improved by SS-31 treatment. We observed reduced treadmill running time in old mice compared to young mice, and our old mice treated with SS-31 for 8 weeks ran significantly longer than old control mice (Fig. 1f), consistent with recent observations [16].

SS-31 treatment suppresses mitochondrial ROS production in old cardiomyocytes

The SS-31 peptide has been shown to attenuate mitochondrial oxidative stress in multiple disease models [9, 12, 17]. To investigate its effect on mitochondrial ROS production in cardiomyocytes, we isolated cardiomyocytes from old control and old SS-31 treated mice and measured mitochondrial ROS production with fluorescent indicators of ROS. Confocal microscopy revealed reduced mitoSOX intensity in cardiomyocytes from old SS-31 treated mice, indicating reduced mitochondrial superoxide production (Fig. 2a), as well as reduced MitoPY1 fluorescence, a measure of mitochondrial hydrogen peroxide production (Fig. 2b).

Increased mitochondrial proton leak in old cardiomyocytes is normalized by SS-31 treatment

To determine the effect of SS-31 treatment on mitochondrial respiration, we assessed the oxygen consumption rate (OCR) in isolated adult cardiomyocytes using the Seahorse Bioscience XF Cell Mito Stress Test assay. Basal respiration was significantly higher in cardiomyocytes from old control mice compared to cardiomyocytes from young mice, and this age-related increase in basal respiration was normalized in cardiomyocytes from old SS-31 treated mice (Fig. 2c, d). These changes in basal respiration were almost entirely the result of altered proton leak, which increased in old cardiomyocytes and was normalized by SS-31 treatment (Fig. 2c, e). In addition, the respiratory control ratio (RCR) decreased in old cardiomyocytes, and this was partially restored by SS-31 treatment. We also measured mitochondrial membrane potential in old cardiomyocytes treated with SS-31, as measured with the dye JC-1 (Supp. Fig. 1). We found increased membrane potential in cardiomyocytes from old SS-31 treated mice, which is consistent with the observed decreased proton leak. We tested whether the improved RCR and reduced proton leak in SS-31 were accompanied by changes in levels of respiratory chain (RC) complexes; however, we observed no change in abundance of subunits of RC complexes after 8-week SS-31 treatment (Fig. 3).

SS-31 treatment reduces protein oxidation and cellular senescence in old hearts

Mitochondrial oxidative stress can lead to oxidative modifications of cellular proteins. We studied whether the extent of Cys S-glutathionylation, an important reversible oxidative posttranslational modification in response to oxidative stress [18], was affected by aging or SS-31 treatment. Overall, proteins in young control hearts have an average of 5.33% occupancy by glutathionylation; this increased by 33% to 7.09% occupancy in old control hearts, but 8-week SS-31 treatment reduced the glutathionylation occupancy of old heart proteins to 5.85%. At the individual peptide level, cardiac proteins from old control mice have increased levels of glutathionylation in the majority of detected peptides compared to young controls, indicating a general age-related increase in protein glutathionylation, substantially and broadly reduced by

SS-31 treatment (Fig. 4a). We also assessed levels of protein carbonylation, another protein oxidative modification, often viewed as a hallmark of oxidative damage [19, 20]. We detected an increase in protein carbonylation in old control compare to young hearts, and this age-related increase was reversed by SS-31 treatment (Fig. 4b).

It has been demonstrated that mitochondrial dysfunction can induce cellular senescence [21]. To determine if the improved mitochondrial respiration and reduced oxidative stress in old SS-31 treated mice was associated with reduced cellular senescence, we examined cellular senescence by immunostaining of senescent markers, p16 and p19, in hearts of old control and old SS-31 treated mice. And indeed, there were fewer senescence cells with p16-positive nuclei or p19-positive nuclei in the SS-31 treated old hearts (Fig. 4c).

SS-31 treatment partially restored aging-induced changes in the proteome and metabolome

We performed global proteomic analyses by mass spectrometry to study the changes in protein abundance induced by SS-31 treatment. We detected 277 proteins with altered expression levels with aging ($q<0.05$ for old controls compared to young controls) and 192 proteins with altered levels in old mice after 8 weeks of SS-31 treatment ($q<0.05$ for old SS-31 compared to old controls) (Fig. S1a). Expression levels of 88 proteins were significantly altered by both aging and SS-31 treatment, and SS-31 attenuated the aging-induced changes for a majority of these proteins (Fig 5). The Ingenuity Pathway Analysis (IPA, https://www.qiagenbioinformatics.com/products/ingenuity-pathway-analysis/) top canonical pathways affected by both aging and SS-31 included mitochondrial dysfunction, oxidative phosphorylation, GP6 signaling pathway and sirtuin signaling pathway ($p<2.8E-06$). However, in comparison with results previously reported for SS-31 treatment in hypertensive heart failure [10], these changes were much smaller in magnitude. We also performed targeted metabolic profiling on cardiac tissue from young and old mice with SS-31 or saline treatment. Out of the 160 metabolites measured, 112 metabolites were detected in all samples and the levels of 18 metabolites were significantly different among the groups ($q<0.05$, Fig. S2a). Age-related reductions in levels were significant in 11 of the 18 metabolites and while none of these were significantly different between old control and old SS-31 groups, SS-31 partially attenuated these age-related metabolic changes (Fig. S2a). Enrichment analysis was performed to gain biological insight into the age-related metabolic changes and showed that metabolites in aspartate metabolism and urea cycle were enriched (Fig S2b).

SS-31 treatment normalized age-related hypo-phosphorylation of cMyBP-C at Ser282

Myofilament proteins are important regulators of cardiac muscle contraction and relaxation. Phosphorylation of myofilament proteins modulates myofilament properties and regulates the relaxation behavior of cardiac muscle [22]. More specifically, phosphorylation of cardiac myosin binding protein C (cMyBP-C) can modulate cross-bridge detachment and diastolic function [23]. Old hearts displayed hypo-phosphorylation of MyBP-C at Ser282, and SS-31 treatment normalized this age-related decrease in cMyBP-C Ser282 phosphorylation (Fig. 6a), consistent with its association with improved relaxation. Cardiac troponin I (cTnI) is an inhibitory subunit of troponin, and phosphorylation of cTnI has been shown to increase the rate of cardiac relaxation [24]. Phosphorylation of Ser23/24 and Ser150 of cTnI was not altered in old murine hearts, and SS-31 treatment had no effect on Ser23/24 and Ser150 phosphorylation (Fig. 6b and c). Titin is a giant myofilament protein in the sarcomere and titin isoform ratio (N2BA/N2B ratio) can modulate passive myocardial and diastolic function [25]. However, we observed no changes in N2BA/N2B ratio with SS-31 treatment (Fig 6d).

Late-life mCAT expression also improved diastolic function and SS-31 treatment cannot further improve cardiac function in old mCAT mice

To determine if reducing mtROS in late-life is sufficient to rescue age-related cardiac dysfunction, we administered an adeno-associated virus serotype-9 vector expressing mitochondrial-targeted catalase (AAV9-mCAT) [26] to old C57Bl6 mice to induce expression of catalase in cardiac mitochondria. We observed improved diastolic function at 8 and 12 weeks after AAV9-mCAT administration (Fig. 7a), suggesting that late-life reduction of mtROS is sufficient to initiate the molecular changes required to reverse age-related diastolic dysfunction. Life-long expression of mCAT was previously shown to prevent age-related mitochondrial ROS accumulation and substantially attenuate declines in cardiac function in old mCAT mice [7]. To determine if SS-31 treatment would have additive impact on mCAT mice, we administered SS-31 to old mCAT mice, but observed no further improvement in diastolic function and myocardial performance at up to 8 weeks (Fig. 7b, c), although the SS-31 induced improvement in diastolic function and myocardial performance seen previously in old wild-type mice was fully recapitulated. These results suggest that the cardiac benefits induced by SS-31 and mCAT are mechanistically overlapping.

SS-31 treatment and mCAT expression have differential effects on myofilament protein phosphorylation

To investigate the mechanism by which SS-31 improves diastolic function, we assessed how late-life mCAT expression altered phosphorylation of myofilament proteins. Unlike SS-31, late-life mCAT expression resulted in small reduction in Ser282 phosphorylation of cMyBP-C (Fig. 8a). Interestingly, late-life mCAT expression increased phosphorylation of cTnI at Ser23/24 and Ser150 (Fig. 8b and c), which may contribute to the improved diastolic function. While SS-31 treatment and mCAT expression have differential effects on regulation of myofilament protein phosphorylation, both interventions mediate improved diastolic function in old mice.

Discussion

Mitochondrial dysfunction is a hallmark of aging and has been implicated in the pathogenesis of cardiovascular diseases. We tested the hypothesis that pharmacologic targeting of mitochondrial dysfunction in late-life can reverse age-related cardiac dysfunction in mice. The main findings of the study are: 1) enhancing mitochondrial function at late-life by administration of mitochondrial-targeted SS-31 peptide or AAV-mediated expression of mitochondrial targeted catalase can reverse pre-existing cardiac dysfunction in old mice; 2) SS-31 treatment normalizes the age-related increase in mitochondrial proton leak, reduces ROS production by old cardiomyocytes, and reduces protein oxidative modifications; 3) the rescue of diastolic function by SS-31 in old mice is due, at least in part, to reversal of phosphorylation of key myofilament proteins; and 4) SS-31 treatment and mCAT expression, while similar in many ways, differentially regulate myofilament protein phosphorylation. These findings are summarized in a proposed mechanistic model of how SS-31 improves mitochondrial function and regulates myofilament properties to improve cardiomyocytes relaxation and reversing age-related cardiac dysfunction (Fig. 9).

Targeting mitochondrial oxidative stress in late-life reverses cardiac aging phenotypes

Transgenic mCAT expression reduces mitochondrial oxidative stress and attenuates cardiac aging phenotypes in mice [7]. While life-long mCAT expression has many positive effects [13], including prevention of pressure-overload induced cardiac hypertrophy or failure [8, 11] and

attenuating the decline in cardiac function during aging [7], there may be negative pleotropic effects at young age [27]. For this, and practical reasons, a treatment that can be started at old age to reverse cardiac aging is a much more desirable therapeutic strategy. Here, we demonstrated that both SS-31 treatment and mCAT expression starting at late-life can reverse the age-related decline in diastolic function. This result suggests that reducing mitochondrial oxidative stress at late-life can be sufficient to initiate molecular changes, including phosphorylation of myofilament proteins, to improve diastolic function.

SS-31 (elamipretide) is a tetrapeptide with an alternating aromatic-cationic amino acids motif that is selectively enriched in mitochondria [28]. Although SS-31 was initially thought to be a mitochondrial targeted antioxidant [29, 30], it has more recently been shown to interact with cardiolipin to enhance inner membrane cristae curvature and function of the electron transport chain (ETC), including the electron carrying activity of cyt c, while reducing cyt c peroxidase activity [31-33]. SS-31 has been shown to enhance ATP levels and endurance in aged skeletal muscle [34]. SS-31 has also been shown to provide similar protection as mCAT in models of pressure overload-induced cardiac hypertrophy and failure [9, 10], however, whether SS-31 treatment is protective against cardiac aging had not been previously established. We found that the reversal of cardiac aging phenotypes by late-life SS-31 treatment was accompanied by reduced oxidative protein modifications in aged hearts, which can be explained by the reduced mitochondrial superoxide and hydrogen peroxide production in SS-31 treated cardiomyocytes. As shown in Fig. 9, SS-31 and mCAT both reduce ROS, however, the former is believed to do so by prevention of ROS production, while the latter directly scavenges hydrogen peroxide. Both, however, will inhibit the vicious cycle of ROS induced damage to mitochondrial DNA and proteins and prevent pathological ROS-Induced-Redox Signaling. Consistent with this overlap, SS-31 treatment cannot further improve the cardiac function of old mCAT mice (Fig. 7b and c), supporting the role of reduction of mitochondrial oxidative stress as a key mechanism of SS-31 reversal of cardiac aging. As noted below, however, this doesn't rule out the involvement of other molecular mechanisms, especially those that may be due to direct augmentation of mitochondrial ATP production by SS-31.

A recent study by Cieslik and colleagues showed that combined treatment with glutathione precursors, N-Acetyl Cysteine (NAC) and Glycine, but not NAC alone, can reverse age-related diastolic dysfunction [35]. While the study suggests that aged mice may benefit from increased glutathione content, the effects of the combined treatment on *in vivo* cardiac glutathione contents and S-glutathionylation remain to be established. Here, we showed that SS-31 can reverse diastolic dysfunction and normalized the age-related increase in protein S-glutathionylation without the necessity to exogenously alter glutathione levels. This supports the primary importance of reducing mitochondrial ROS in redox homeostasis. In addition, the fact that SS-31 treatment or late-life mCAT expression can reverse age-related diastolic dysfunction but NAC alone fails to do so supports the importance of mitochondrial localization of the ROS combating action in cardiac aging protection.

Normalization of proton leak in aged cardiomyocytes is a protective mechanism of SS-31

Mitochondrial oxidative phosphorylation is the major source of ATP production in the cell. When electrons from substrate oxidation pass through electron transport chain complexes, the energy generated is used to pump protons from mitochondrial matrix to the intermembrane space to generate a proton gradient. The resulting protonmotive force drives protons back to mitochondrial matrix through ATP synthase, while converting ADP to ATP. However, this coupling of substrate oxidation and ATP synthesis is incomplete as protons can also re-enter mitochondrial matrix independent of ATP synthesis in a process termed "proton leak" [36]. In this study, we showed that cardiomyocytes from old mice exhibited increased proton leak when

compared to cardiomyocytes from young mice. This age-related increase in proton leak is consistent with previous observations that aging increases proton leak in mouse hepatocytes and in mitochondria from rat heart, kidney and liver [37, 38]. Strikingly, 8-week treatment with SS-31 completely reversed the age-related increase in mitochondrial proton leak in cardiomyocytes (Fig 2c and e).

While the molecular mechanisms of proton leak are not fully understood, it has been shown that basal leak through mitochondrial inner membrane or around inner membrane proteins, and inducible leak through adenine nucleotide translocase (ANT) or uncoupling proteins (UCPs) contribute to mitochondrial proton leak [36]. Because SS-31 interacts with cardiolipin in the inner mitochondrial membrane, it is possible that SS-31 can regulate basal leak by preserving inner membrane integrity and normalizing the function of inner membrane spanning proteins. ROS has been shown to induce mitochondrial uncoupling and increase proton leak [39-41], and thus, reduced ROS production following SS-31 treatment may also contribute to the lowered proton leak. A protective function of ROS-induced proton leak has been suggested, where increased ROS level promotes proton leak to reduce mitochondrial membrane potential and decrease further ROS production and oxidative damage [39]. However, the reduced RCR and increased oxidative damage seen in the aged heart suggest that this increased proton leak is maladaptive and a result of compromised mitochondria function. In addition to suppressing proton leak, SS-31 partially restores the RCR and increases mitochondrial membrane potential in aged cardiomyocytes, suggesting that SS-31 treatment reverses age-related mitochondrial dysfunction. It has been shown that mitochondrial dysfunction induces cellular senescence, and PolG mutator mice, which have increased mtDNA mutation and mtROS, also have accumulation of senescent cells [21]. Compared to old controls, SS-31 treated hearts have reduced numbers of p16- or p19-positive senescent cells and this may be a direct result of the restoration of mitochondrial function [21].

SS-31 and mCAT expression differentially regulate phosphorylation of myofilament proteins to improve diastolic function

SS-31 treatment reduces cardiac dysfunction in models of pressure-overload induced heart failure, and this is accompanied by marked proteomic changes [10]. In comparison, however, SS-31 induces more modest changes in protein expression in the aging heart (Fig. 5), and no changes in expression of ETC subunits (Fig. 3). In this study, we also investigated the effect of SS-31 treatment on the cardiac metabolite profile and detected modest changes in metabolite levels, with SS-31 treatment showing a tendency of attenuation of the age-related metabolic changes.

On the other hand, post-translational modifications, both oxidative and phosphorylative, may play a more important role in conferring the benefits of SS-31 treatment. In cardiac muscle, the state of post-translational modifications of myofilament proteins are crucial to the regulation of contractile and relaxation behaviors, as shown in the pathophysiology of heart failure [42-44]. In particular, phosphorylation of myofilament proteins is a key modulator of diastolic function of the heart [43, 45, 46]. cMyBP-C is a sarcomeric protein that modulates actin–myosin interaction and cross-bridge cycling. It is a critical mediator of diastolic function whose activity has been shown to be regulated by phosphorylation of its cardiac specific M-domain [23, 46]. Previous studies have shown that a high level of phosphorylation is critical to normal cardiac function, and hypo-phosphorylation of the M-domain is associated with heart failure [47-49]. Ser282 is one of the phosphorylation sites in the M-domain. Sadayappan and colleagues showed that Ser282 phosphorylation is critical for subsequent phosphorylation of Ser302, another phosphorylation site in the M-domain of cMyBP-C, and phospho-ablation at Ser282 impairs baseline diastolic function and response to β-adrenergic stimulation [50]. We detected an age-related decrease in

phosphorylation of S282 in the M-domain of cMyBP-C, and SS-31 treatment restores Ser282 phosphorylation in old mice, likely contributing to the restoration of diastolic function.

TnI is an inhibitory subunit of troponin, and it binds to actin to inhibit actomyosin interaction in the absence of calcium binding to TnC [51]. Phosphorylation of cTnI at Ser23/24 by protein kinase A has been shown to reduce myofilament Ca^{2+} sensitivity and increase myofilament relaxation rate [24, 52]. Biesiadecki lab recently showed simultaneous increases in Ser23/24 and Ser150 phosphorylation in ischemic hearts and suggested that this combined phosphorylation plays an adaptive role in ischemia by maintaining Ca^{2+} sensitivity and accelerating Ca^{2+} dissociation [53, 54]. Late-life mCAT expression, but not SS-31, increased phosphorylation of TnI at Ser23/24 and Ser150. The effects of these increases in cTnI phosphorylation on Ca^{2+} sensitivity and myofilament relaxation in aging cardiac muscles remain to be investigated. Unlike SS-31 treatment, late-life mCAT expression fails to increase Ser282 phosphorylation of cMyBP-C. Although reduction of mtROS is a shared protective mechanism between SS-31 and mCAT, it is likely that the two interventions activate different kinases to regulate myofilament protein phosphorylation to mediate improved relaxation in the aging hearts. Future *ex vivo* biomechanical assays are required to determine how the two interventions differentially regulate cross-bridge kinetics and Ca^{2+} sensitivity to improve diastolic function.

In conclusion, this study demonstrated that late-life SS-31 treatment can reverse pre-existing cardiac aging phenotypes, including diastolic dysfunction. Besides reducing mitochondrial ROS production and oxidative damage, SS-31 treatment reduces the age-related increase in mitochondrial proton leak in cardiomyocytes. Despite similar cardiac benefits, SS-31 and mCAT expression induced differential changes in myofilament protein phosphorylation, in line with overlapping but not concordant mechanisms of action. These results support the therapeutic potential of targeting mitochondrial dysfunction to reverse the effects of cardiac aging.

Methods

Animals

Young (3-5-month-old) and old (24-month-old) C57BL/6 male and female mice were obtained from the National Institute of Aging Charles River colony. Mice were housed at 20ºC in an AAALAC accredited facility under Institutional Animal Care Committee supervision.

For each sex, old mice were randomly assigned to two groups and SS-31 (3 ug/g body weight/day; kindly provided by Stealth BioTherapeutics, Newton, MA) or saline-vehicle were delivered subcutaneously via osmotic minipumps (Alzet 1004) for 4 weeks. After 4-week, the original minipump was surgically removed and a new minipump was implanted to continue the SS-31 or saline-vehicle delivery for another 4 weeks. For evaluation of persistent effects of SS-31 treatment, the minipump was surgically removed after 8-week treatment.

To study the effect of reducing mtROS at late-life, recombinant AAV9 vector expressing a mitochondria-targeted catalase gene (AAV9-mCAT) was delivered to 24-month-old WT C57BL/6 female mice by retro-orbital injection. A total of 5×10^{12} vg particles of AAV were delivered to each mouse [26]. Retro-orbital injection of saline was performed as control.

To study the interaction of SS-31 and catalase, 23- to 27-month-old mCAT mice and age-matched WT littermates were given 8-week subcutaneous delivery of SS-31 (3 ug/g body weight/day) or saline-vehicle via minipumps.

Echocardiography was performed at baseline and post-treatment timepoints to evaluate systolic and diastolic function of the mice. Mouse was anesthetized by 0.5-1% isoflurane and echocardiogram was performed using a Siemens Acuson CV-70 equipped with a 13MHz probe.

For treadmill running, mice were acclimated to the treadmill for 2 consecutive days before the measurement. At the day of measurement, mice were placed on the treadmill at a 10° incline when the treadmill accelerated from 0 m/min to 30 m/min in a 5 min period, and allowed to run to exhaustion at 30 m/min. Exhaustion was determined if the mice fail to remount the treadmill after receiving 5 consecutive shocks and light physical prodding. Treadmill measurements were performed during the natural active period of the mice between 8 pm and 2 am.

At the endpoint, mice were euthanized by cervical dislocation. The heart was immediately removed, weighed and processed for downstream analyses.

Cardiomyocyte isolation and respiration measurement

Ventricular myocytes were enzymatically isolated from the hearts of C57BL/6 mice using a protocol modified from that described previously [55]. Briefly, the animal was euthanized by cervical dislocation. The heart was immediately removed from the chest, raised and perfused with oxygenated modified Ca2+ free-Tyrode's solution for 5 min. Then the heart was perfused with 50 ml low Ca2+ solution containing 300U/ml collagenase II + 0.5mg/ml hyaluronidase at 37ºC for 20 - 30 min. The ventricle was cut into small pieces and further digested under gentle agitation. Rod shaped adult cardiomyocytes were collected by settling down of cells and plated in 24 well plates for XF24e Extracellular Flux Analyzer analysis (Seahorse Bioscience) or on glass coverslips for confocal imaging.

Cardiomyocyte imaging

For confocal imaging, we used modified Tyrode's solution (in mM: 138 NaCl, 0.5 KCl, 20 HEPES, 1.2 MgSO4, 1.2 KH2PO4, 1 CaCl2, 5 Glucose, pH 7.4) and a Leica SP8 (Leica, Germany) inverted confocal microscope for confocal imaging at room temperature. For mitochondrial superoxide quantitation, we used the ratio of MitoSOX Red (5 μM, excited at 540 nm and emissions collected at >560 nm) to mitoTrackerGreen (200nM, excited at 488nm and emission collected at 505-530 nm). For mitochondrial H2O2 measurement, we used the ratio of MitoPY1 (5μM, excited at 488 nm and emission collected at 520 - 640 nm) and MitoDeepRed (100nM, excited at 633nm and emission collected > 660 nm). For mitochondrial membrane potential measurement, JC-1 was excited by 488 nm laser and emission collected at 510 - 545 nm and 570 - 650 nm.

Cardiomyocyte respiration measurement

For intact cardiomyocyte respiration measurement, 800 cardiomyocytes were plated in each well of XF24e Extracellular Flux Analyzer 24 well plates (Seahorse Bioscience) and mitochondrial respiration was assessed in 3 hours after plating. Mitochondrial respiration was assessed using the Seahorse Bioscience XF Cell Mito Stress Test assay, with OCR values measured at baseline and after the sequential addition of 1 μM oligomycin, 0.5 mM FCCP and 1 μM rotenone +1 μM antimycin A [56]. The OCR values for basal respiration, proton leak, ATP turnover, maximum respiration and non-mitochondrial respiration were thereby determined. Respiratory control ratio (RCR) was calculated as the ratio of maximum respiration to proton leak.

Immunoblotting

Proteins were extracted from frozen heart tissues with K150T buffer (150 mM KCl, 50 mM Tris-HCl pH7.4, 0.125% Na deoxycholate, 0.375%Triton X-100, 0.15% NP-40, 4mM EDTA, 50 mM NaF) and quantified by BCA protein assay (Thermo Scientific). Equal amount of proteins (15 ug) were resolved on 4-12% NuPAGE Bis-Tris gel and transferred to PVDF membrane. A Pierce Reversible Protein Stain Kit was used to detect total proteins for normalization of loading.

Primary antibodies used in immunoblotting were OXPHOS (Abcam ab110413, at 1:500), Troponin I (Cell Signaling Technology #4002, 1:1000), pSer23/24-Troponin I (Cell Signaling Technology #4004, 1:1000), pSer150-Troponin I (ThermoFisher PA5-35410), cMyBP-C (Santa Cruz SC-137237, 1:1000), pSer282-cMyBP-C (ALX-215-057-R050, 1:2000).

Secondary antibodies used were donkey anti-rabbit IgG secondary antibody and goat anti-mouse IgG secondary antibody (both from Thermo Scientific). AlphaView Software (Protein Simple, San Jose, CA), was used for image acquisition and quantification.

Measurement of protein S-glutathionylation

Quantification of protein-S-glutathionylation was performed using an established redox proteomics workflow [57]. Briefly, nine heart samples (young, aged with SS-31 treatment, and aged control, n = 3 for each) were subjected to protein extraction, selective reduction and enrichment, trypsin digestion and isobaric labeling with tandem mass tags 10-plex. For occupancy analysis, the levels of total thiol were quantified in a pooled sample. Mass spectrometry was performed on a Q Exactive Plus (Thermo Fisher Scientific), and data processing was conducted as previously described [57].

Protein carbonyl assay

Protein carbonyl levels in heart tissues were measured using OxiSelect protein carbonyl ELISA kit (Cell Biolabs, San Diego, CA) according to the manufacturer's instructions.

Metabolite profiling measurement

Pulverized cardiac tissues were homogenized in 200 ul of water and 800 ul of methanol were added to the homogenates. The homogenates were incubated on dry ice for 30 min and then sonicated in ice water bath for 10 min. The homogenates were centrifuged at 13000 rpm at 4ºC for 5 min and the soluble extracts were dried by speed vac. The extracts were reconstituted and analyzed by LC-MS as described [15].

The results of metabolite profiling were analyzed using Metaboanalyst 4.0 [58]. The relative peak intensities of metabolites were median normalized, log transformed and auto-scaled. One-way ANOVA was used for comparisons among all groups and Tukey's HSD was used for pairwise comparisons. A heatmap was generated for all metabolites with significantly different levels among groups (FDR<0.05) For the 11 metabolites that showed age-related changes in levels ($p<0.05$ by Tukey's HSD), enrichment analysis was performed by Metaboanalyst 4.0 using the Pathway-associated metabolite sets as library.

Immunohistochemistry

Hearts were fixed overnight in 4% paraformaldehyde, paraffin embedded and 4 µm sections deparaffinized, treated with ethylenediamine tetraacetic acid (EDTA) buffer pH 8 and incubated with rabbit anti-p16 antibody (1:300, Abcam ab211542) or anti-p19 antibody (1:300, LSBio LS-

C49180), Seattle, WA) overnight at 4 ºC. Secondary antibody detection was performed with ImmPRESS VR Anti-Rabbit IgG HRP Polymer Detection Kit (Vector Laboratories, Burlingame, CA), developed with diaminobenzidine (Sigma-Aldrich, St. Louis, MO) and counterstained with Mayer's Hematoxylin (Sigma-Aldrich, St. Louis, MO). Positive nuclear stain was expressed as a percentage of p16 positive or p19 positive nuclei (brown) versus total nuclei (brown + blue).

Mass spectrometry for proteomic analysis

Pulverized heart tissues were homogenized in ice-cold extraction buffer (250 mM sucrose, 1 mM EGTA, 10 mM HEPES, 10 mM Tris-HCl pH7.4). Lysates were centrifuged at 800 x g for 10 minutes to remove debris. Samples were trypsin digested and purified by MCX column (Waters). LC-MS/MS analysis was performed with a Waters nanoAcquity UPLC and a Thermo Scientific Q Exactive mass spectrometer. Topograph software was used for peptide abundance measurement as previously described [15]. The statistical analysis of relative protein abundance between experimental groups were performed using a linear model of peptide abundance to calculate fold changes of proteins between experimental groups using the R/Bioconductor software. The p-values were adjusted for multiple comparison with the Bioconductor package q-value [15]. In order to generate the heatmap, we computed a z-score of the average log2-abundance, where we adjusted the data, by protein, to have a mean of zero and a standard deviation of 1. The heatmap was generated using the Complex Heatmap (v.1.20.0) R package. We used IPA (https://www.qiagenbioinformatics.com/products/ingenuity-pathway-analysis/) to identify pathways that were significantly altered by both aging and SS-31 treatment within the dataset.

Measurement of Titin isoforms

Relative expression of N2B and N2BA isoforms of titin were assessed in heart tissues using a vertical SDS-agarose gel system as previously described [59, 60]. The ratio of intensities of N2BA band and N2B band were then determined.

Statistical analyses

Echocardiographic results were analyzed by paired T-test with baseline and linear regression over time. Results of cardiomyocyte imaging were analyzed by T-test compared to old saline control. HW/Tibia, mitochondrial respiration, real-time PCR and immunoblotting results were analyzed by one-way ANOVA with SNK or Dunnett's post hoc analysis. Graphpad Prism 5 and Prism 8 were used for statistical analyses and all data were plotted as mean±SEM. Results of metabolite profiling and proteomic analysis were analyzed as described in above sections.

Figure legends

Figure 1. **SS-31 treatment reverses cardiac aging phenotypes and improves exercise performance in old mice.** Doppler echocardiography showed that 8-week SS-31 treatment (A) improved diastolic function (increased Ea/Aa) and (B) enhanced myocardial performance (reduced myocardial performance index, MPI) of old mice. (C) Fractional shortening (FS) was not altered by SS-31 treatment. (A-C) *p<0.05 to corresponding 0-week baseline; p<0.05 linear regression over time for Ea/Aa and MPI of SS-31 treated mice; n=7/group. (D) 8-week SS-31 treatment regressed the age-related increase in normalized heart weight. *p<0.05 vs. young saline; #p<0.05 vs. old saline; n=8-10/group. (E) The improved diastolic function (increased Ea/Aa) after 8-week of SS-31 treatment persisted for 2-4 weeks after cessation of treatment.

n=7/group (F) Treadmill running was impaired in old control mice but was rescued by SS-31 treatment. *p<0.05 vs. young saline; #p<0.05 vs. old saline; n≥9/group.

Figure 2. **SS-31 treatment reduces ROS production and improves respiration in cardiomyocytes.** (A) SS-31 treated cardiomyocyte showed reduced mitochondrial superoxide, indicated by mitoSox (normalized to mitochondrial content by the ratio to mitotracker green), compared to old controls. *p<0.05 vs old saline; n=3 mice/group. (B) After SS-31 treated cardiomyocyte showed reduced hydrogen peroxide, indicated by mitoPY1 (normalized to mitochondrial content using mito deep red), compared to old controls. *p<0.05 vs old saline; n=3 mice/group. (C) Averaged traces of oxygen consumption rate (OCR, +/- SEM) of isolated cardiomyocytes from young, old, and old SS-31 treated mice measured by the Seahorse XF Cell Mito Stress Test. (D-E) Cardiomyocytes from old mice exhibited increased basal respiration (D) and proton leak (E) compared to that of young mice, and these age-related increases were reversed in cardiomyocytes from 8-week SS-31 treated old mice. (F) Old cardiomyocytes exhibited reduced respiratory control ratio (RCR) compared to young cardiomyocytes and this decrease was partially restored by 8-week SS-31 treatment. n≥17/group. (D-F) *p<0.05 vs. young saline; #p<0.05 vs. old saline; n=17-35 from 3-6 mice.

Figure 3. **SS-31 treatment does not alter expression of subunits of oxidative phosphorylation complexes.** Immunoblotting using anti- OXPHOS antibody detected no differences in expression levels of OXPHOS subunits (NDUFB8, SDHB, UQCRC2, MTCO1, and ATP5A) in hearts of old mice treated with 8 weeks of SS-31 treatment. Transient changes in NDUFB8 levels were detected at 1 and 2 weeks after SS-31 treatment. *p<0.05 vs Control; +p<0.05 vs 1-week SS-31; #p<0.05 vs 2-week SS-31 treatment; n≥5/group.

Figure 4. **SS-31 treatment reduces protein oxidation and senescence in old hearts.** (A) A histogram of the distribution of changes in glutathionylation levels in peptides from old control and old SS-31 treated hearts. n≥6/group. (B) Increased levels of protein carbonylation were detected in hearts of old control, but not old SS-31 treated, mice when compared to young control mice. *p<0.05 vs young; n=5/group. (C) IHC staining of cellular senescence markers, p16 (left panel) and p19 (right panel), detected reduced p16 and p19 positive nuclei in old SS-31 treated heart compared to old control hearts. *p<0.05 vs old saline; n=5/group.

Figure 5. **SS-31 treatment partially restores age-related proteomic remodeling**. A heatmap of the 88 proteins that were significantly altered by both aging (q<0.05 for old control vs. young control and SS-31 treatment (q<0.05 for old SS-31 vs. old control); n≥8/group. Row labels on the right are the UniProtID_GeneID of each protein. The identity and fold change of each protein are described in supplemental Table 1.

Figure 6. **SS-31 rescues the age-related hypo-phosphorylation of MyBP-C.** (A) Old murine hearts displayed reduced levels of MyBP-C phosphorylation at Ser282, which is normalized by SS-31 treatment; *p<0.05 vs. young; #p<0.05 vs. old; n≥5/group. (B-C) Aging and SS-31 treatment did not alter phosphorylation of cTnI at Ser23/24 (B) and Ser150 (C) in old hearts; n≥5/group. (D) Titin isoform ratio (N2BA/N2B ratio) did not change with SS-31 treatment; n=6-8/group.

Figure 7. **The cardiac benefit of SS-31 treatment is not additive to the cardiac benefit of mCAT expression.** (A) Diastolic function (Ea/Aa) improved at both 8 and 12 weeks after AAV9-mCAT administration. n=3-6/group. (B) SS-31 improved diastolic function in old WT but did not further improve the function of old mCAT mice. (C) SS-31 improved myocardial performance (reduced MPI) in old WT but did not further improve the performance of old mCAT mice.

*p<0.05 compared to baseline by paired t-test; significant regression statistics were indicated in figures; n=3-6/group.

Figure 8. **SS-31 treatment and mCAT expression differentially regulate myofilament protein phosphorylation.** (A) Late-life mCAT expression reduced Ser282 phosphorylation of MyBP-C. (B-C) Late-life mCAT expression increased phosphorylation of cTnI at Ser23/24 (B) and Ser150 (C). *p<0.05 vs. saline controls; n≥3/group.

Figure 9. **Schematic outline of results and interpretation.** While mCAT and SS-31 both inhibit electron transport chain produced ROS, they do so by different mechanisms. Both inhibit a ROS-mediated vicious cycle (ROS induced mtDNA and protein damage leads to greater ROS generation; striped arrows) and ROS-Induced redox signaling. However, by promoting electron transport, preventing proton leakage and augmenting ATP production, SS-31 also improves mitochondrial energetics. By improving mitochondrial energetics and reducing pathologic redox signaling, SS-31 promotes phosphorylation of cMyBP-C to enhance myofilament relaxation kinetics, while mCAT expression does so through phosphorylation of cTnI.

Figure S1. **SS-31 treatment increases mitochondrial membrane potential in aged cardiomyocytes.** *p<0.05 vs old saline. n=18-19/group.

Figure S2. **SS-31 treatment induces modest changes in metabolome that partially attenuates the age-related changes.** (A) A heat map of the relative levels of the 18 metabolites that were significantly (FDR<0.05) different among treatment groups. n≥8/group. (B) A network of metabolite set enrichment for the 11 metabolites that were significantly (p<0.05, by Tukey's HSD) altered by aging.

Acknowledgements

The authors wish to acknowledge Stealth BioTherapeutics (Newton, MA) for kindly providing the SS-31 peptide. We thank Jeanne Fredrickson her assistance in biochemical assay and the Northwest Metabolomics Research Center (NW-MRC) for metabolomics service. We acknowledge funding support from Glenn/AFAR Postdoctoral Fellowship for Translational Research on Aging, NIA 5T32AG000057 Training Grant support and NIA K99 AG051735 to YAC and NIA P01 AG001751 and P30 AG013280 to PSR.

Competing interests

The authors declare no competing interest.

Materials & Correspondence

Correspondence to: Peter S. Rabinovitch, MD, PhD; E-mail: petersr@u.washington.edu

References

1. Lopez-Otin C, Blasco MA, Partridge L, Serrano M and Kroemer G. The hallmarks of aging. *Cell*. 2013;153:1194-217.
2. Harman D. The biologic clock: the mitochondria? *J Am Geriatr Soc*. 1972;20:145-7.
3. Niccoli T and Partridge L. Ageing as a risk factor for disease. *Curr Biol*. 2012;22:R741-52.

4. Lakatta EG and Levy D. Arterial and cardiac aging: major shareholders in cardiovascular disease enterprises: Part I: aging arteries: a "set up" for vascular disease. *Circulation*. 2003;107:139-46.
5. Tocchi A, Quarles EK, Basisty N, Gitari L and Rabinovitch PS. Mitochondrial dysfunction in cardiac aging. *Biochim Biophys Acta*. 2015;1847:1424-33.
6. Schriner SE, Linford NJ, Martin GM, Treuting P, Ogburn CE, Emond M, Coskun PE, Ladiges W, Wolf N, Van Remmen H, Wallace DC and Rabinovitch PS. Extension of murine life span by overexpression of catalase targeted to mitochondria. *Science*. 2005;308:1909-11.
7. Dai DF, Santana LF, Vermulst M, Tomazela DM, Emond MJ, MacCoss MJ, Gollahon K, Martin GM, Loeb LA, Ladiges WC and Rabinovitch PS. Overexpression of catalase targeted to mitochondria attenuates murine cardiac aging. *Circulation*. 2009;119:2789-97.
8. Dai DF, Johnson SC, Villarin JJ, Chin MT, Nieves-Cintron M, Chen T, Marcinek DJ, Dorn GW, 2nd, Kang YJ, Prolla TA, Santana LF and Rabinovitch PS. Mitochondrial Oxidative Stress Mediates Angiotensin II-Induced Cardiac Hypertrophy and G{alpha}q Overexpression-Induced Heart Failure. *Circ Res*. 2011;108:837-46.
9. Dai DF, Chen T, Szeto H, Nieves-Cintron M, Kutyavin V, Santana LF and Rabinovitch PS. Mitochondrial targeted antioxidant Peptide ameliorates hypertensive cardiomyopathy. *J Am Coll Cardiol*. 2011;58:73-82.
10. Dai DF, Hsieh EJ, Chen T, Menendez LG, Basisty NB, Tsai L, Beyer RP, Crispin DA, Shulman NJ, Szeto HH, Tian R, MacCoss MJ and Rabinovitch PS. Global proteomics and pathway analysis of pressure-overload-induced heart failure and its attenuation by mitochondrial-targeted peptides. *Circ Heart Fail*. 2013;6:1067-76.
11. Dai DF, Hsieh EJ, Liu Y, Chen T, Beyer RP, Chin MT, MacCoss MJ and Rabinovitch PS. Mitochondrial proteome remodelling in pressure overload-induced heart failure: the role of mitochondrial oxidative stress. *Cardiovasc Res*. 2012;93:79-88.
12. Dai DF, Chiao YA, Marcinek DJ, Szeto HH and Rabinovitch PS. Mitochondrial oxidative stress in aging and healthspan. *Longev Healthspan*. 2014;3:6.
13. Dai DF, Chiao YA, Martin GM, Marcinek DJ, Basisty N, Quarles EK and Rabinovitch PS. Mitochondrial-Targeted Catalase: Extended Longevity and the Roles in Various Disease Models. *Prog Mol Biol Transl Sci*. 2017;146:203-241.
14. Chiao YA, Ramirez TA, Zamilpa R, Okoronkwo SM, Dai Q, Zhang J, Jin YF and Lindsey ML. Matrix metalloproteinase-9 deletion attenuates myocardial fibrosis and diastolic dysfunction in ageing mice. *Cardiovasc Res*. 2012;96:444-55.
15. Dai DF, Karunadharma PP, Chiao YA, Basisty N, Crispin D, Hsieh EJ, Chen T, Gu H, Djukovic D, Raftery D, Beyer RP, MacCoss MJ and Rabinovitch PS. Altered proteome turnover and remodeling by short-term caloric restriction or rapamycin rejuvenate the aging heart. *Aging Cell*. 2014;13:529-39.
16. Campbell MD, Duan J, Samuelson AT, Gaffrey MJ, Wang L, Bammler TK, Moore RJ, White CC, Kavanagh TJ, Voss JG, Szeto HH, Rabinovitch PS, Qian WJ and Marcinek DJ. Improving mitochondrial function with SS-31 reverses age-related redox stress and improves exercise tolerance in aged mice. *Free Radic Biol Med*. 2018.
17. Tarantini S, Valcarcel-Ares NM, Yabluchanskiy A, Fulop GA, Hertelendy P, Gautam T, Farkas E, Perz A, Rabinovitch PS, Sonntag WE, Csiszar A and Ungvari Z. Treatment with the mitochondrial-targeted antioxidant peptide SS-31 rescues neurovascular coupling responses and cerebrovascular endothelial function and improves cognition in aged mice. *Aging Cell*. 2018;17.
18. Shelton MD and Mieyal JJ. Regulation by reversible S-glutathionylation: molecular targets implicated in inflammatory diseases. *Mol Cells*. 2008;25:332-46.
19. Dalle-Donne I, Rossi R, Giustarini D, Milzani A and Colombo R. Protein carbonyl groups as biomarkers of oxidative stress. *Clin Chim Acta*. 2003;329:23-38.

20. Fedorova M, Bollineni RC and Hoffmann R. Protein carbonylation as a major hallmark of oxidative damage: update of analytical strategies. *Mass Spectrom Rev*. 2014;33:79-97.
21. Wiley CD, Velarde MC, Lecot P, Liu S, Sarnoski EA, Freund A, Shirakawa K, Lim HW, Davis SS, Ramanathan A, Gerencser AA, Verdin E and Campisi J. Mitochondrial Dysfunction Induces Senescence with a Distinct Secretory Phenotype. *Cell Metab*. 2016;23:303-14.
22. Biesiadecki BJ, Davis JP, Ziolo MT and Janssen PML. Tri-modal regulation of cardiac muscle relaxation; intracellular calcium decline, thin filament deactivation, and cross-bridge cycling kinetics. *Biophys Rev*. 2014;6:273-289.
23. Tong CW, Nair NA, Doersch KM, Liu Y and Rosas PC. Cardiac myosin-binding protein-C is a critical mediator of diastolic function. *Pflugers Arch*. 2014;466:451-7.
24. Zhang R, Zhao J, Mandveno A and Potter JD. Cardiac troponin I phosphorylation increases the rate of cardiac muscle relaxation. *Circ Res*. 1995;76:1028-35.
25. Nagueh SF, Shah G, Wu Y, Torre-Amione G, King NM, Lahmers S, Witt CC, Becker K, Labeit S and Granzier HL. Altered titin expression, myocardial stiffness, and left ventricular function in patients with dilated cardiomyopathy. *Circulation*. 2004;110:155-62.
26. Li D, Lai Y, Yue Y, Rabinovitch PS, Hakim C and Duan D. Ectopic catalase expression in mitochondria by adeno-associated virus enhances exercise performance in mice. *PLoS One*. 2009;4:e6673.
27. Basisty N, Dai DF, Gagnidze A, Gitari L, Fredrickson J, Maina Y, Beyer RP, Emond MJ, Hsieh EJ, MacCoss MJ, Martin GM and Rabinovitch PS. Mitochondrial-targeted catalase is good for the old mouse proteome, but not for the young: 'reverse' antagonistic pleiotropy? *Aging Cell*. 2016;15:634-45.
28. Szeto HH. Cell-permeable, mitochondrial-targeted, peptide antioxidants. *AAPS J*. 2006;8:E277-83.
29. Belin RJ, Sumandea MP, Allen EJ, Schoenfelt K, Wang H, Solaro RJ and de Tombe PP. Augmented protein kinase C-alpha-induced myofilament protein phosphorylation contributes to myofilament dysfunction in experimental congestive heart failure. *Circ Res*. 2007;101:195-204.
30. Cho S, Szeto HH, Kim E, Kim H, Tolhurst AT and Pinto JT. A novel cell-permeable antioxidant peptide, SS31, attenuates ischemic brain injury by down-regulating CD36. *J Biol Chem*. 2007;282:4634-42.
31. Birk AV, Chao WM, Bracken C, Warren JD and Szeto HH. Targeting mitochondrial cardiolipin and the cytochrome c/cardiolipin complex to promote electron transport and optimize mitochondrial ATP synthesis. *Br J Pharmacol*. 2014;171:2017-28.
32. Birk AV, Liu S, Soong Y, Mills W, Singh P, Warren JD, Seshan SV, Pardee JD and Szeto HH. The mitochondrial-targeted compound SS-31 re-energizes ischemic mitochondria by interacting with cardiolipin. *J Am Soc Nephrol*. 2013;24:1250-61.
33. Szeto HH. First-In-Class Cardiolipin Therapeutic to Restore Mitochondrial Bioenergetics. *Br J Pharmacol*. 2013.
34. Siegel MP, Kruse SE, Percival JM, Goh J, White CC, Hopkins HC, Kavanagh TJ, Szeto HH, Rabinovitch PS and Marcinek DJ. Mitochondrial-targeted peptide rapidly improves mitochondrial energetics and skeletal muscle performance in aged mice. *Aging Cell*. 2013;12:763-71.
35. Cieslik KA, Sekhar RV, Granillo A, Reddy A, Medrano G, Heredia CP, Entman ML, Hamilton DJ, Li SM, Reineke E, Gupte AA, Zhang AJ and Taffet GE. Improved Cardiovascular Function in Old Mice After N-Acetyl Cysteine and Glycine Supplemented Diet: Inflammation and Mitochondrial Factors. *J Gerontol a-Biol*. 2018;73:1167-1177.
36. Jastroch M, Divakaruni AS, Mookerjee S, Treberg JR and Brand MD. Mitochondrial proton and electron leaks. *Essays Biochem*. 2010;47:53-67.
37. Harper ME, Monemdjou S, Ramsey JJ and Weindruch R. Age-related increase in mitochondrial proton leak and decrease in ATP turnover reactions in mouse hepatocytes. *Am J Physiol*. 1998;275:E197-206.

38. Serviddio G, Bellanti F, Romano AD, Tamborra R, Rollo T, Altomare E and Vendemiale G. Bioenergetics in aging: mitochondrial proton leak in aging rat liver, kidney and heart. *Redox Rep*. 2007;12:91-5.
39. Brookes PS. Mitochondrial H(+) leak and ROS generation: an odd couple. *Free Radic Biol Med*. 2005;38:12-23.
40. Brookes PS, Land JM, Clark JB and Heales SJ. Peroxynitrite and brain mitochondria: evidence for increased proton leak. *J Neurochem*. 1998;70:2195-202.
41. Echtay KS, Roussel D, St-Pierre J, Jekabsons MB, Cadenas S, Stuart JA, Harper JA, Roebuck SJ, Morrison A, Pickering S, Clapham JC and Brand MD. Superoxide activates mitochondrial uncoupling proteins. *Nature*. 2002;415:96-9.
42. Biesiadecki BJ. Myofilament modulation of contraction. *Arch Biochem Biophys*. 2016;601:1-3.
43. Hamdani N, Bishu KG, von Frieling-Salewsky M, Redfield MM and Linke WA. Deranged myofilament phosphorylation and function in experimental heart failure with preserved ejection fraction. *Cardiovasc Res*. 2013;97:464-71.
44. Ramirez-Correa GA, Martinez-Ferrando MI, Zhang P and Murphy AM. Targeted proteomics of myofilament phosphorylation and other protein posttranslational modifications. *Proteomics Clin Appl*. 2014;8:543-53.
45. Hamdani N, Franssen C, Lourenco A, Falcao-Pires I, Fontoura D, Leite S, Plettig L, Lopez B, Ottenheijm CA, Becher PM, Gonzalez A, Tschope C, Diez J, Linke WA, Leite-Moreira AF and Paulus WJ. Myocardial titin hypophosphorylation importantly contributes to heart failure with preserved ejection fraction in a rat metabolic risk model. *Circ Heart Fail*. 2013;6:1239-49.
46. Rosas PC, Liu Y, Abdalla MI, Thomas CM, Kidwell DT, Dusio GF, Mukhopadhyay D, Kumar R, Baker KM, Mitchell BM, Powers PA, Fitzsimons DP, Patel BG, Warren CM, Solaro RJ, Moss RL and Tong CW. Phosphorylation of cardiac Myosin-binding protein-C is a critical mediator of diastolic function. *Circ Heart Fail*. 2015;8:582-94.
47. Copeland O, Sadayappan S, Messer AE, Steinen GJ, van der Velden J and Marston SB. Analysis of cardiac myosin binding protein-C phosphorylation in human heart muscle. *J Mol Cell Cardiol*. 2010;49:1003-11.
48. Jacques AM, Copeland O, Messer AE, Gallon CE, King K, McKenna WJ, Tsang VT and Marston SB. Myosin binding protein C phosphorylation in normal, hypertrophic and failing human heart muscle. *J Mol Cell Cardiol*. 2008;45:209-16.
49. Kooij V, Holewinski RJ, Murphy AM and Van Eyk JE. Characterization of the cardiac myosin binding protein-C phosphoproteome in healthy and failing human hearts. *J Mol Cell Cardiol*. 2013;60:116-20.
50. Sadayappan S, Gulick J, Osinska H, Barefield D, Cuello F, Avkiran M, Lasko VM, Lorenz JN, Maillet M, Martin JL, Brown JH, Bers DM, Molkentin JD, James J and Robbins J. A critical function for Ser-282 in cardiac Myosin binding protein-C phosphorylation and cardiac function. *Circ Res*. 2011;109:141-50.
51. Gomes AV, Potter JD and Szczesna-Cordary D. The role of troponins in muscle contraction. *IUBMB Life*. 2002;54:323-33.
52. Kentish JC, McCloskey DT, Layland J, Palmer S, Leiden JM, Martin AF and Solaro RJ. Phosphorylation of troponin I by protein kinase A accelerates relaxation and crossbridge cycle kinetics in mouse ventricular muscle. *Circ Res*. 2001;88:1059-65.
53. Nixon BR, Walton SD, Zhang B, Brundage EA, Little SC, Ziolo MT, Davis JP and Biesiadecki BJ. Combined troponin I Ser-150 and Ser-23/24 phosphorylation sustains thin filament Ca(2+) sensitivity and accelerates deactivation in an acidic environment. *J Mol Cell Cardiol*. 2014;72:177-85.
54. Salhi HE, Hassel NC, Siddiqui JK, Brundage EA, Ziolo MT, Janssen PM, Davis JP and Biesiadecki BJ. Myofilament Calcium Sensitivity: Mechanistic Insight into TnI Ser-23/24 and Ser-150 Phosphorylation Integration. *Front Physiol*. 2016;7:567.

55. Zhang H, Shang W, Zhang X, Gu J, Wang X, Zheng M, Wang Y, Zhou Z, Cao JM, Ji G, Zhang R and Cheng H. Beta-adrenergic-stimulated L-type channel Ca(2)+ entry mediates hypoxic Ca(2)+ overload in intact heart. *J Mol Cell Cardiol*. 2013;65:51-8.
56. Zhang H, Wang P, Bisetto S, Yoon Y, Chen Q, Sheu SS and Wang W. A novel fission-independent role of dynamin-related protein 1 in cardiac mitochondrial respiration. *Cardiovasc Res*. 2017;113:160-170.
57. Kramer PA, Duan J, Gaffrey MJ, Shukla AK, Wang L, Bammler TK, Qian W-J and Marcinek DJ. Fatiguing contractions increase protein S-glutathionylation occupancy in mouse skeletal muscle. *Redox biology*. 2018;17:367-376.
58. Chong J, Soufan O, Li C, Caraus I, Li S, Bourque G, Wishart DS and Xia J. MetaboAnalyst 4.0: towards more transparent and integrative metabolomics analysis. *Nucleic Acids Res*. 2018;46:W486-W494.
59. Tonino P, Kiss B, Strom J, Methawasin M, Smith JE, 3rd, Kolb J, Labeit S and Granzier H. The giant protein titin regulates the length of the striated muscle thick filament. *Nat Commun*. 2017;8:1041.
60. Warren CM, Jordan MC, Roos KP, Krzesinski PR and Greaser ML. Titin isoform expression in normal and hypertensive myocardium. *Cardiovasc Res*. 2003;59:86-94.

Figure 1.

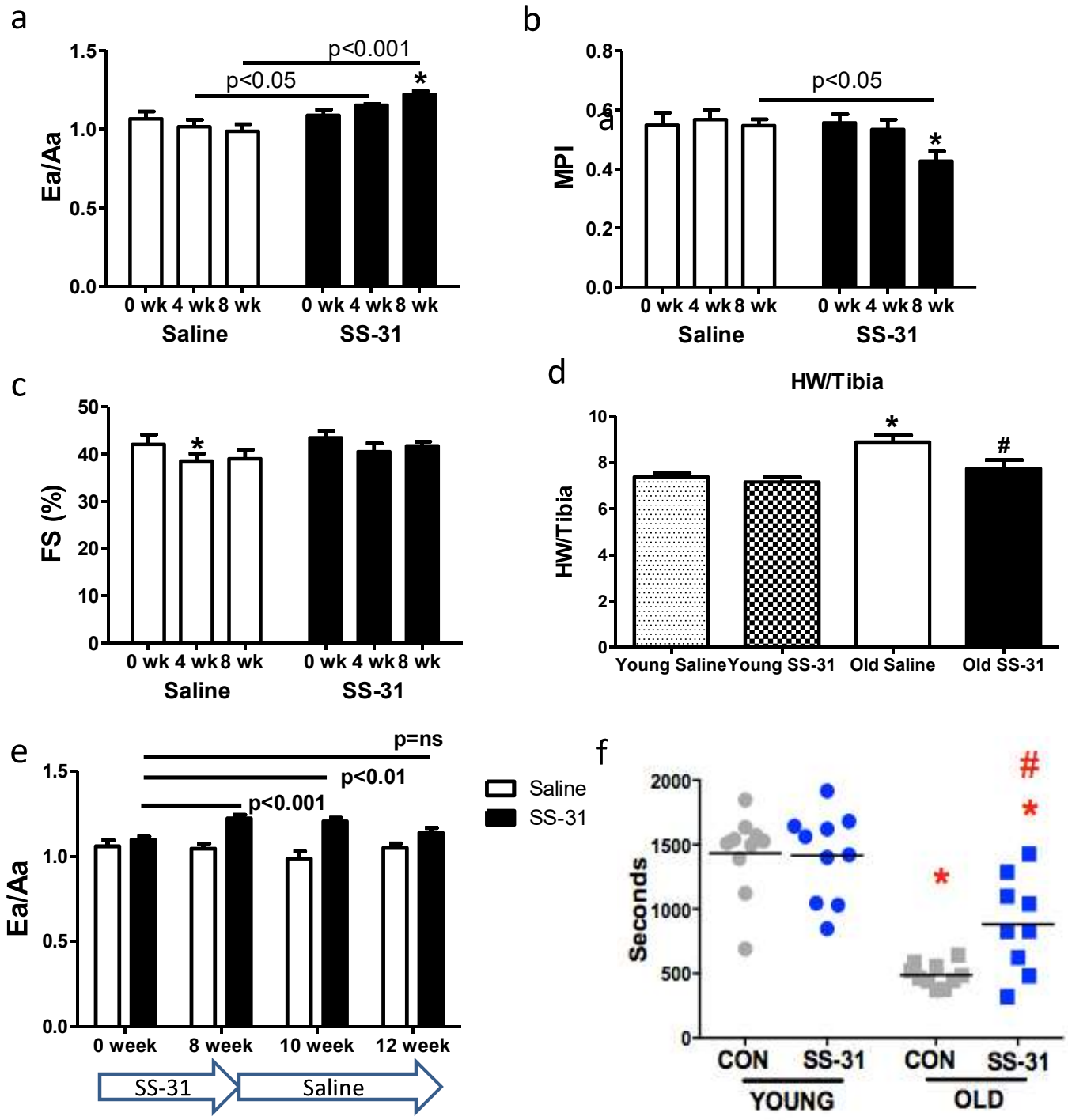
a
p<0.001
p<0.05
*
Ea/Aa
1.5
1.0
0.5
0.0
0 wk 4 wk 8 wk
0 wk 4 wk 8 wk
Saline
SS-31
b
p<0.05
a
*
MPI
0.8
0.6
0.4
0.2
0.0
0 wk 4 wk 8 wk
0 wk 4 wk 8 wk
Saline
SS-31
c
*
FS (%)
50
40
30
20
10
0
0 wk 4 wk 8 wk
0 wk 4 wk 8 wk
Saline
SS-31
d
HW/Tibia
*
#
HW/Tibia
10
8
6
4
2
0
Young Saline
Young SS-31
Old Saline
Old SS-31
e
p=ns
p<0.01
p<0.001
Ea/Aa
1.5
1.0
0.5
0.0
0 week
8 week
10 week
12 week
SS-31
Saline
Saline
SS-31
f
#
*
*
Seconds
2000
1500
1000
500
0
CON
SS-31
CON
SS-31
YOUNG
OLD

Figure 2.

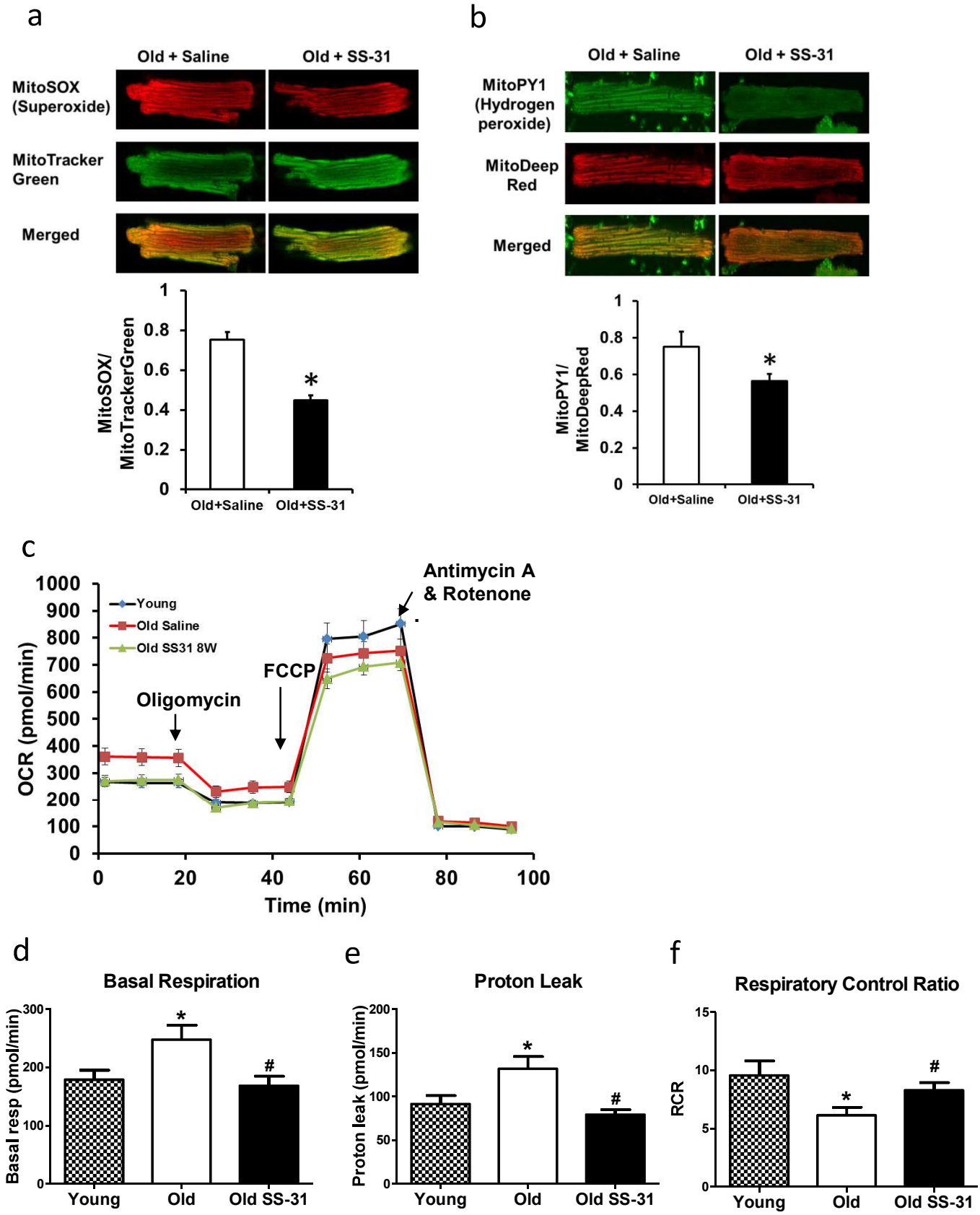
a
Old + Saline
Old + SS-31
MitoSOX (Superoxide)
MitoTracker Green
Merged
MitoSOX/ MitoTrackerGreen
Old+Saline
Old+SS-31
b
MitoPY1 (Hydrogen peroxide)
MitoDeep Red
MitoPY1/ MitoDeepRed
c
Young
Old Saline
Old SS31 8W
Antimycin A & Rotenone
FCCP
Oligomycin
OCR (pmol/min)
Time (min)
d
Basal Respiration
Basal resp (pmol/min)
Young
Old
Old SS-31
e
Proton Leak
Proton leak (pmol/min)
f
Respiratory Control Ratio
RCR

Figure 3.

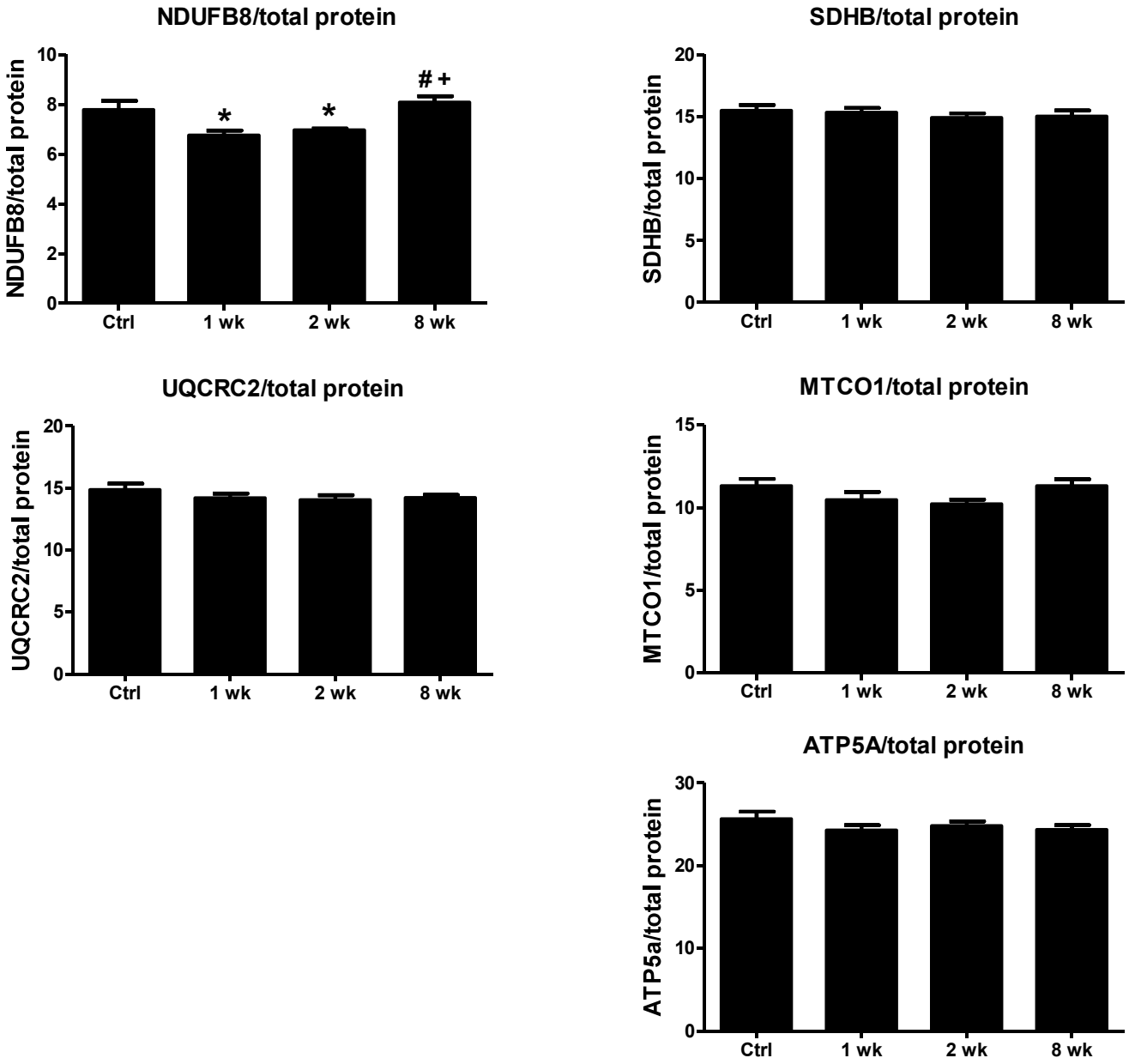
NDUFB8/total protein
NDUFB8/total protein
10
8
6
4
2
0
*
*
+
Ctrl
1 wk
2 wk
8 wk
SDHB/total protein
SDHB/total protein
20
15
10
5
0
Ctrl
1 wk
2 wk
8 wk
UQCRC2/total protein
UQCRC2/total protein
20
15
10
5
0
Ctrl
1 wk
2 wk
8 wk
MTCO1/total protein
MTCO1/total protein
15
10
5
0
Ctrl
1 wk
2 wk
8 wk
ATP5A/total protein
ATP5a/total protein
30
20
10
0
Ctrl
1 wk
2 wk
8 wk

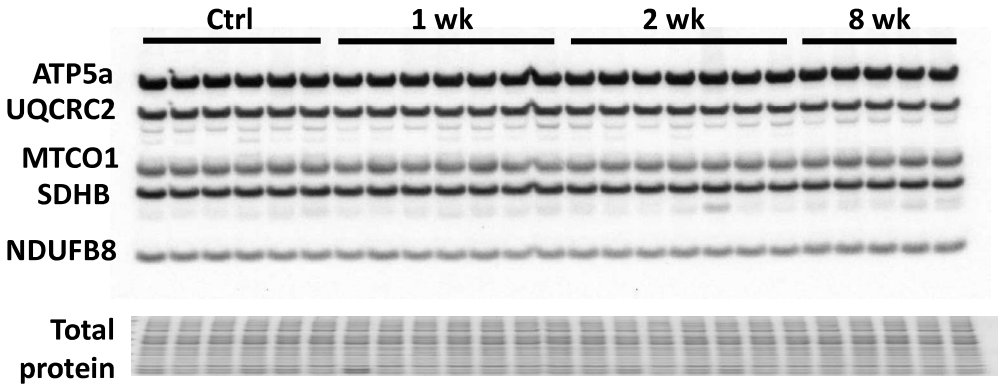
Ctrl
1 wk
2 wk
8 wk
ATP5a
UQCRC2
MTCO1
SDHB
NDUFB8
Total protein

Figure 4.

a

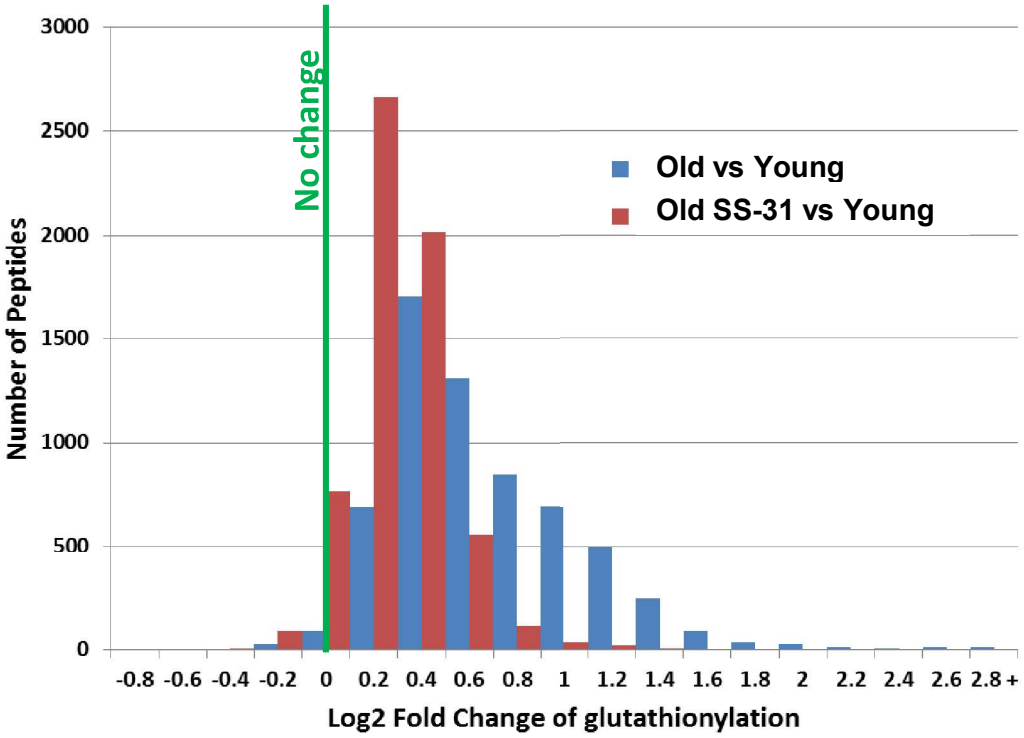
No change
Old vs Young
Old SS-31 vs Young
Number of Peptides
3000
2500
2000
1500
1000
500
0
-0.8 -0.6 -0.4 -0.2 0 0.2 0.4 0.6 0.8 1 1.2 1.4 1.6 1.8 2 2.2 2.4 2.6 2.8 +
Log2 Fold Change of glutathionylation

b

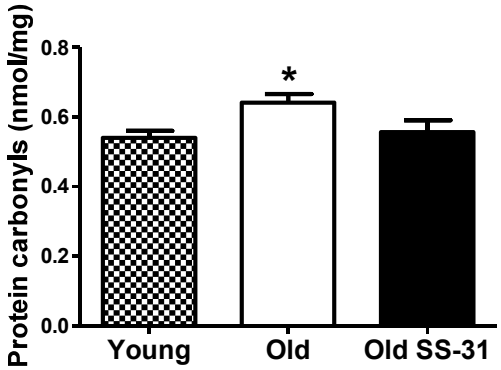
Protein carbonyls (nmol/mg)
0.8
0.6
0.4
0.2
0.0
*
Young
Old
Old SS-31

c

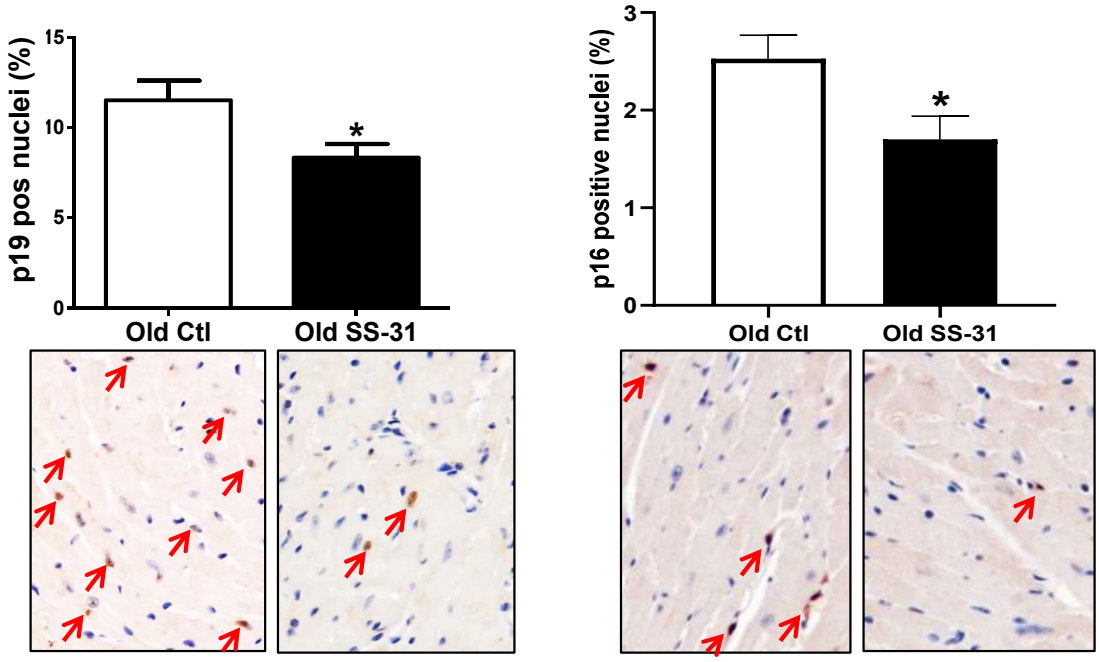
p19 pos nuclei (%)
15
10
5
0
*
Old Ctl
Old SS-31
p16 positive nuclei (%)
3
2
1
0
*
Old Ctl
Old SS-31

Figure 5.

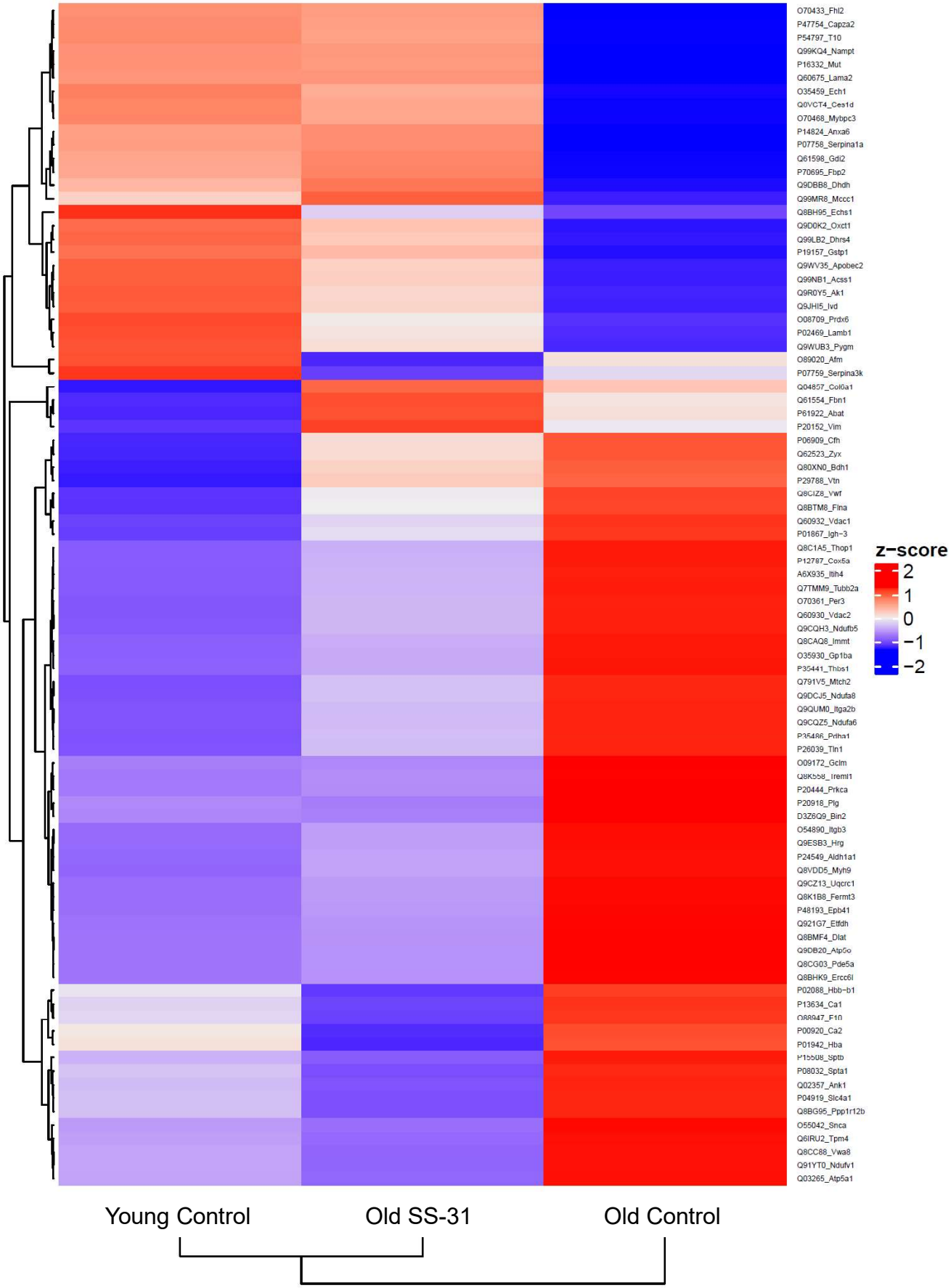
O70433_Fhl2
P47754_Capza2
P54797_T10
Q99KQ4_Nampt
P16332_Mut
Q60675_Lama2
O35459_Ech1
Q0VCT4_Ces1d
O70468_Mybpc3
P14824_Anxa6
P07758_Serpina1a
Q61598_Gdi2
P70695_Fbp2
Q9DBB8_Dhdh
Q99MR8_Mccc1
Q8BH95_Echs1
Q9D0K2_Oxct1
Q99LB2_Dhrs4
P19157_Gstp1
Q9WV35_Apobec2
Q99NB1_Acss1
Q9R0Y5_Ak1
Q9JHI5_Ivd
O08709_Prdx6
P02469_Lamb1
Q9WUB3_Pygm
O89020_Afm
P07759_Serpina3k
Q04857_Col6a1
Q61554_Fbn1
P61922_Abat
P20152_Vim
P06909_Cfh
Q62523_Zyx
Q80XN0_Bdh1
P29788_Vtn
Q8CIZ8_Vwf
Q8BTM8_Flna
Q60932_Vdac1
P01867_Igh−3
Q8C1A5_Thop1
P12787_Cox5a
A6X935_Itih4
Q7TMM9_Tubb2a
O70361_Per3
Q60930_Vdac2
Q9CQH3_Ndufb5
Q8CAQ8_Immt
O35930_Gp1ba
P35441_Thbs1
Q791V5_Mtch2
Q9DCJ5_Ndufa8
Q9QUM0_Itga2b
Q9CQZ5_Ndufa6
P35486_Pdha1
P26039_Tln1
O09172_Gclm
Q8K558_Iremt1
P20444_Prkca
P20918_Plg
D3Z6Q9_Bin2
O54890_Itgb3
Q9ESB3_Hrg
P24549_Aldh1a1
Q8VDD5_Myh9
Q9CZ13_Uqcrc1
Q8K1B8_Fermt3
P48193_Epb41
Q921G7_Etfdh
Q8BMF4_Dlat
Q9DB20_Atp5o
Q8CG03_Pde5a
Q8BHK9_Ercc6l
P02088_Hbb−b1
P13634_Ca1
O88947_F10
P00920_Ca2
P01942_Hba
P15508_Sptb
P08032_Spta1
Q02357_Ank1
P04919_Slc4a1
Q8BG95_Ppp1r12b
O55042_Snca
Q6IRU2_Tpm4
Q8CC88_Vwa8
Q91YT0_Ndufv1
Q03265_Atp5a1
z−score
2
1
0
−1
−2
Young Control
Old SS-31
Old Control

Figure 6.

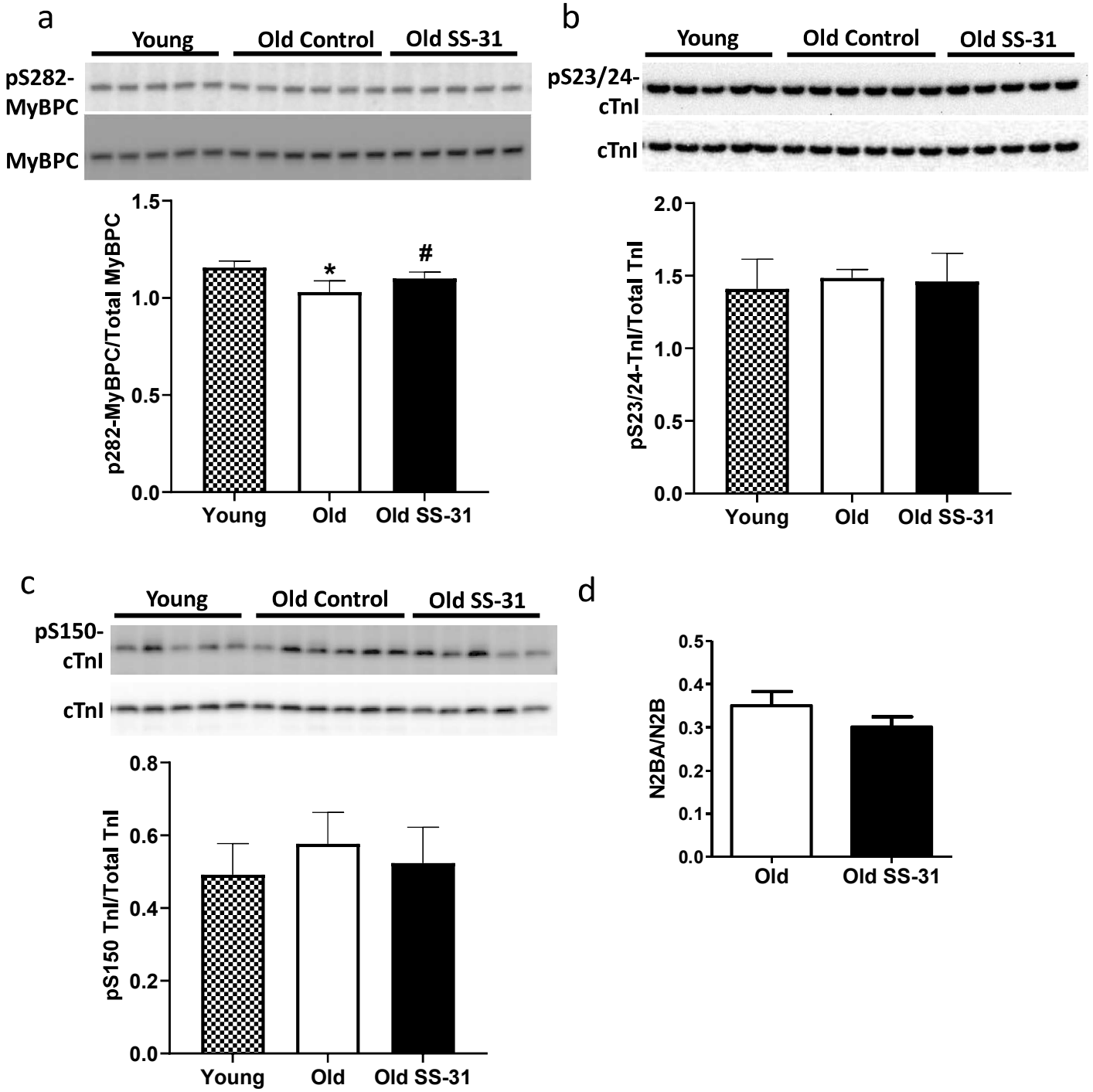
a
Young
Old Control
Old SS-31
pS282-MyBPC
MyBPC
p282-MyBPC/Total MyBPC
1.5
1.0
0.5
0.0
*
#
Young
Old
Old SS-31
b
Young
Old Control
Old SS-31
pS23/24-cTnI
cTnI
pS23/24-TnI/Total TnI
2.0
1.5
1.0
0.5
0.0
Young
Old
Old SS-31
c
Young
Old Control
Old SS-31
pS150-cTnI
cTnI
pS150 TnI/Total TnI
0.8
0.6
0.4
0.2
0.0
Young
Old
Old SS-31
d
N2BA/N2B
0.5
0.4
0.3
0.2
0.1
0.0
Old
Old SS-31

Figure 7.

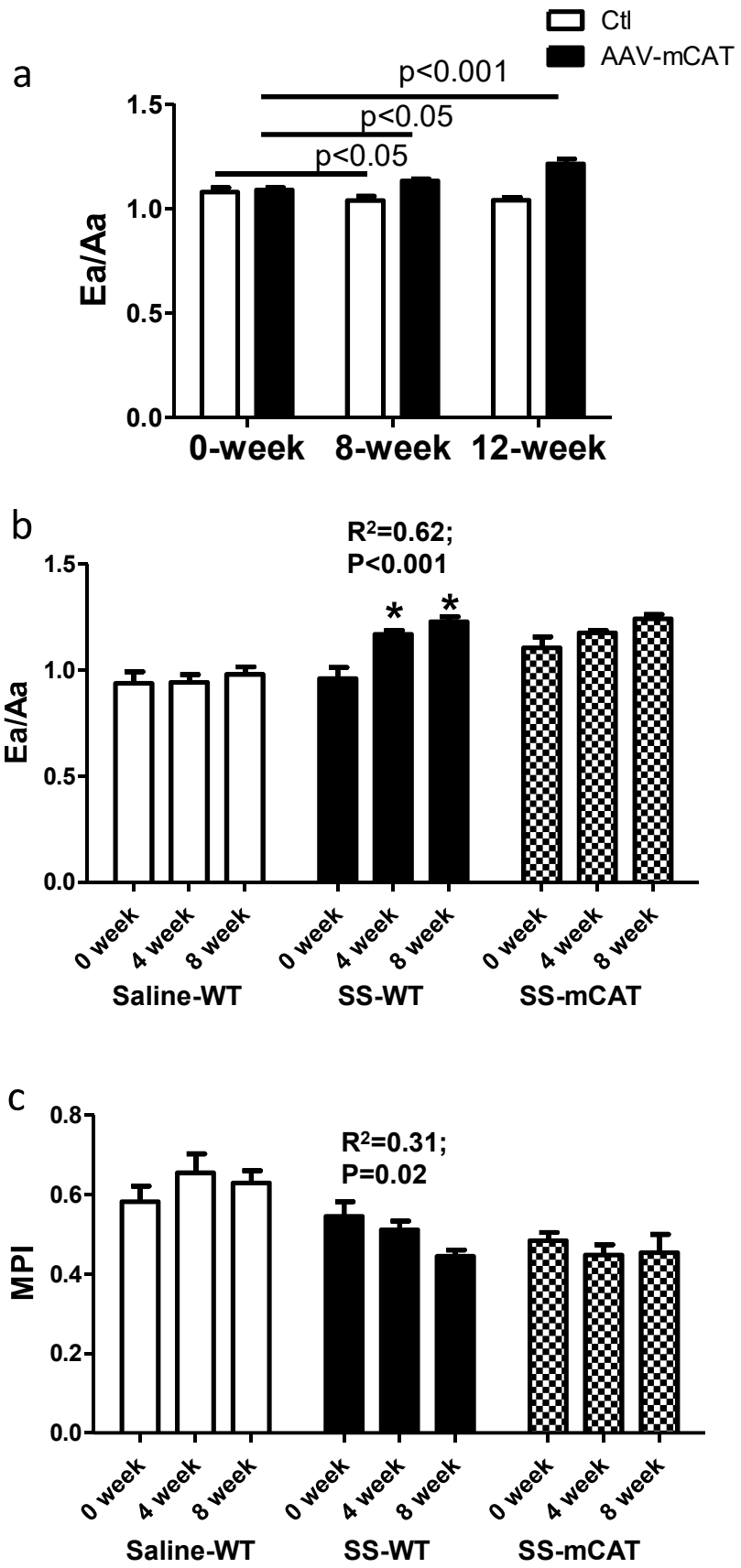
a
Ctl
AAV-mCAT
p<0.001
p<0.05
p<0.05
Ea/Aa
1.5
1.0
0.5
0.0
0-week
8-week
12-week
b
R²=0.62;
P<0.001
*
*
Ea/Aa
1.5
1.0
0.5
0.0
0 week
4 week
8 week
Saline-WT
SS-WT
SS-mCAT
c
R²=0.31;
P=0.02
MPI
0.8
0.6
0.4
0.2
0.0
0 week
4 week
8 week
Saline-WT
SS-WT
SS-mCAT

Figure 8.

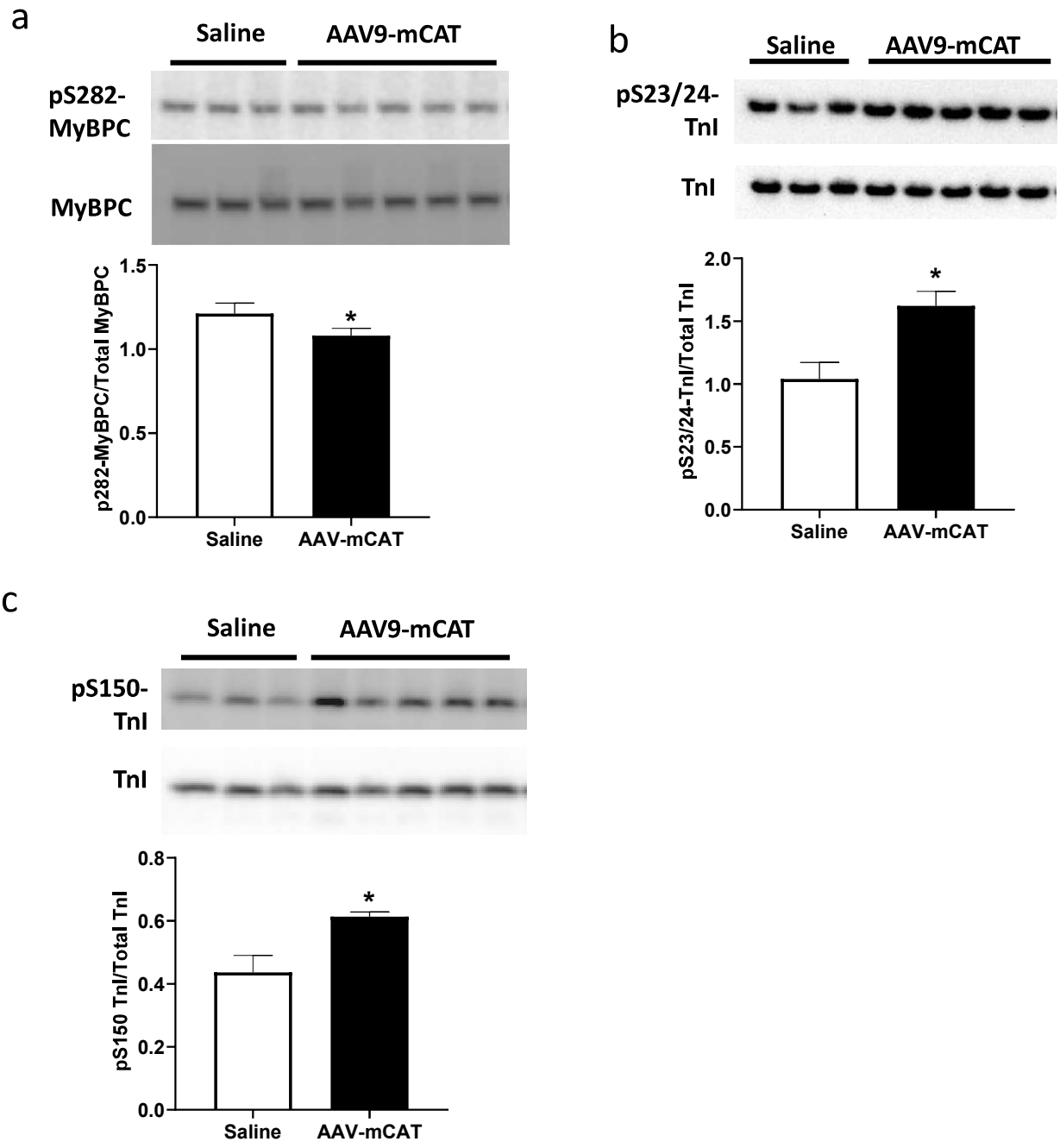
a
Saline
AAV9-mCAT
pS282-MyBPC
MyBPC
p282-MyBPC/Total MyBPC
1.5
1.0
0.5
0.0
*
Saline
AAV-mCAT
b
Saline
AAV9-mCAT
pS23/24-TnI
TnI
pS23/24-TnI/Total TnI
2.0
1.5
1.0
0.5
0.0
*
Saline
AAV-mCAT
c
Saline
AAV9-mCAT
pS150-TnI
TnI
pS150 TnI/Total TnI
0.8
0.6
0.4
0.2
0.0
*
Saline
AAV-mCAT

Figure 9.

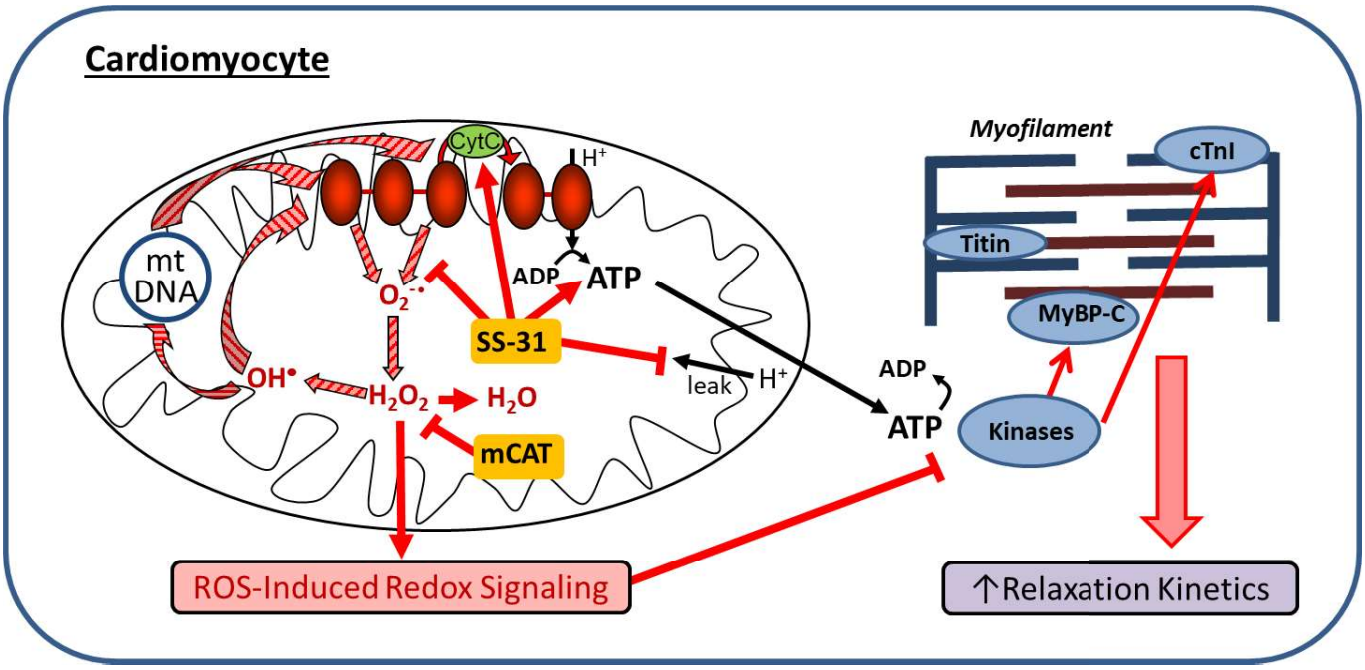
Cardiomyocyte
CytC
H+
mt DNA
ADP
ATP
O2-•
SS-31
OH•
H2O2
H2O
leak
H+
mCAT
ADP
ATP
Kinases
Myofilament
cTnI
Titin
MyBP-C
ROS-Induced Redox Signaling
↑Relaxation Kinetics